

EMISSION INDUCED BY STRONG COUPLING BETWEEN HYBRID TAMM–SURFACE PLASMON POLARITON MODE AND RHODAMINE 6G DYE EXCITON

E. Bužavaitė-Vertelienė^{a,b}, V. Žičkus^a, J. Anulytė^a, and Z. Balevičius^{a,b}

^a*Department of Laser Technologies, Center for Physical Sciences and Technology, Saulėtekio 3, 10257 Vilnius, Lithuania*

^b*Faculty of Electronics, Vilnius Gediminas Technical University, Plytinės 25, 10105 Vilnius, Lithuania*

Email: zigmas.balevicius@ftmc.lt

Received 19 November 2024; accepted 20 November 2024

Total internal reflection ellipsometry (TIRE) and leakage microscopy were applied for the study of photonic-plasmonic nanostructures supporting hybrid Tamm–surface plasmon modes and their strong coupling with Rhodamine 6G organic dye excitons. The optical response of TIRE has shown that Tamm and surface plasmon polaritons interact strongly and the formed hybrid plasmonic mode alters resonances in the energy spectra. Moreover, both TPP (Tamm plasmon polaritons) and SPP (surface plasmon polaritons) components in the hybrid mode are strongly coupled with R6G-PMMA (poly(methyl methacrylate)) layers at the inner and outer interfaces of the 50 nm gold layer, respectively. Leakage microscopy in the back focal plane optical configuration proves the energy transfer of excited emitters through the 50 nm gold layer in the strong coupling regime. Polaritonic emission in the strong coupling has better coherence properties than conventional spontaneous fluorescence emission from pure Rhodamine 6G organic dye molecules.

Keywords: strong coupling, polaritonic emission, plasmonics

1. Introduction

Strong coupling between plasmonic resonances and various emitters such as excitons in organic dyes or photochromic molecules or rare earth metals allow one to transfer energy through tens of nanometre thick metallic layers with decreased metal losses [1–4]. The ability of metals to support plasmonic resonances gives the possibility to overcome the diffraction limit and achieve a high enhancement of electric field at the metal–dielectric interface [5]. Such open cavity has an easy access to the volume in which an emitter can be placed. Plasmonic-photonic cavities that are able to support energy exchange in the strong coupling regime are promising for thresholdless nanolasers [6, 7], ultra-sensitive optical sensing [8, 9], modification of chemical reaction rates [10–12] and quantum information processing [13]. The strong coupling regime is achieved when energy exchange between the light-like mode (plasmonic resonance) and the matter like emitters (organic dye molecules) occurs during the coherent

time [14]. In other words, in such a microscopic system the energy exchange between plasmonic resonance and excitons is faster than the damping rate, and as a result, the hybrid plasmon–exciton polaritonic state is generated [15].

Existence of hybrid modes has been shown between two different plasmonic excitations – surface plasmon polaritons (SPP) and Tamm plasmon polaritons (TPP) [16]. The well-known SPP is a propagated surface electromagnetic mode at the interface of a thin (≈ 50 nm) metal layer and a dielectric. The SPP is a non-radiative electromagnetic mode and in order to excite the SPP waves the glass prism or grating coupler are usually used to match the in-plane wave vectors of incident light and the plasma oscillation in the metal [5]. It should be noted that SPP can be excited only in the p polarization. Another type of electromagnetic surface modes existing between the metal and photonic crystals are the so-called Tamm plasmon polariton [17]. TPPs are optical states similar to the electron states proposed by Tamm [18] that appear in the energy band gap on

the crystal surface. In the case of the photonic crystal, the distributed Bragg reflections (DBR) form the forbidden photonic stop band [19] for photons that resembles the energy band gap of the real crystal. Differently from the propagated SPP, the TPP are non-propagating states and can be excited in p and s polarizations. The TPP have an in-plane wave vector which is less than the wave vector of light in a vacuum, thus, a direct optical excitation of TPP is possible, opposite to the SPP where the light wave vector is always smaller than SPP [20]. When conditions of energy and wave vectors are satisfied for both resonances SPP and TPP, the hybrid TPP–SPP mode excitations can be generated. Such matching can be obtained whenever a glass prism or optical objectives (or other couplers) are optically connected with 1D PC (photonic crystal) on which a thin metal layer is deposited on the top. In such plasmonic-photonic structure, the TPP and SPP resonances exist in a broad range of angles of light incidence. If the dispersion relation curves have a splitting, which is wider than the sum of the both excitations widths, it indicates a strong coupling regime between TPP and SPP and the energy spectra of both plasmonic resonances are altered compared with uncoupled ones [21]. It should be noted that the alteration of the plasmonic resonances in wavelength spectra also indicates the dynamics in time domain at frequencies that correspond to the splitting in the hybrid polaritonic mode [22]. This leads to the coherent exchange of energy between an SPP-emitter and a TPP-emitter when an emitter (organic dye molecules) is placed in close proximity of the metal layer where plasmonic resonance takes place. Pump-probe or fluorescence lifetime spectroscopy was used to investigate the dynamics of SPP oscillations strongly coupled with other emitters [11, 23]. However, the decay times for plasmon modes are about ~ 100 fs, and this means that coherent energy exchange is even shorter [24, 25]. The excited energy transfer between molecules through the distance can be achieved by Dexter transfer [26] when two molecular wave functions overlapped (≈ 1 nm) or by Foster transfer [27, 28] as near-field resonant dipole–dipole interaction (≈ 10 nm). Both interactions are non-radiative; however, the energy transfer distance is very short compared with a simple radiative energy transfer where distances are sufficient, but rather high losses and a low efficiency do not allow a coherent

energy transfer. Meanwhile, plasmonic resonances are electromagnetic states which can have microns of propagation lengths in the VIS–NIR range and can efficiently couple with various emitters, thus being able to transfer energy coherently over tens of nanometres in the strong coupling regime.

In this study, we show that the hybrid TPP–SPP mode can efficiently transfer energy and emit in free space through the 50 nm thick gold layer when inner TPP and outer SPP plasmonic components in the hybrid mode are strongly coupled between each other and with two R6G-PMMA rhodamine dye layers (20 nm thick) placed at both gold layer interfaces.

2. Methods

Two different samples were prepared: (1) the sample without a plasmonic nanostructure (CS/R6G) and (2) the hybrid TPP–SPP mode supporting sample (CS/PC/R6G/Au/R6G). Both samples were formed on a coverslip glass (CS) substrate. The first sample was formed by spin coating (3000 rpm) the prepared solution (3:1) of PMMA polymer and Rhodamine 6G molecules dissolved in ethanol. The concentration of PMMA was $c_m = 36.7$ mg/L and the Rhodamine 6G concentration was $c = 25$ mmol/L ($c_m = 11.78$ g/L). The second structure consisted of a photonic crystal (1D PC) made of 5 alternating TiO_2 (60 nm) and SiO_2 (110 nm) bilayers formed by ion beam sputtering on CS. Further, the previously described R6G layer (20 nm) was spin coated on PC, then the 50 nm Au layer was sputtered (magnetron sputtering) and another R6G layer (20 nm) was spin coated.

The fabricated samples were then characterized by the total internal reflection ellipsometry (TIRE) method with an incorporated 45° prism coupler in a range of 40 – 60° angles of incidence (AOI). The TIRE method measures the reflection intensity ratio between the p and s polarization components (Ψ), and the phase difference between them (Δ) and the ellipsometry setup can be seen in Fig. 1, right, where the sample (with the prism attached to it) is introduced into the optical path of an ellipsometric system. The ellipsometer used for measuring the optical response of the two samples was the dual rotating compensator J. A. Woollam RC2 model, where the light source is a Deuterium/Tungsten lamp (210–1700 nm spectral range).

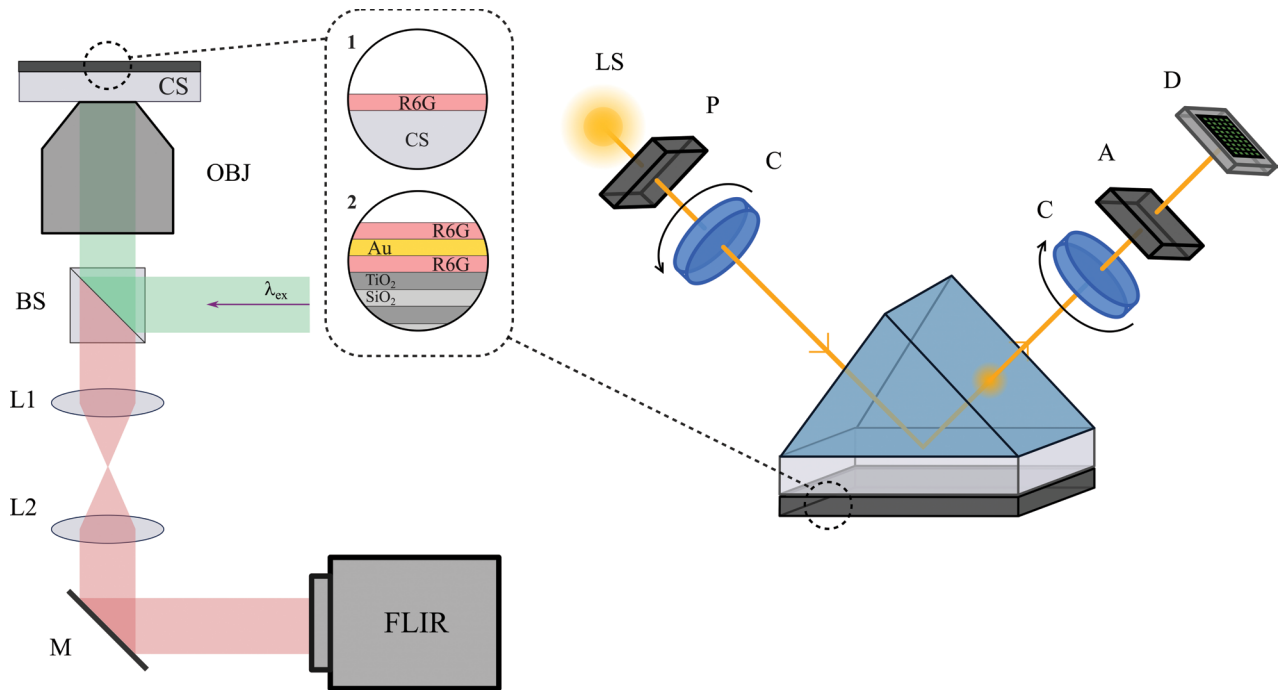


Fig. 1. Total internal reflection fluorescence (TIRF) imaging for back focal plane (BFP) imaging (left) and total internal reflection ellipsometry (right) measuring schemes. The TIRF setup consists of an objective (OBJ), a beam splitter (BS), two convex lenses (L1 and L2), a mirror (M) and an imaging camera (FLIR). The TIRE scheme consists of a white light source (LS), a polarizer (P), two rotating compensators (C), an analyzer (A) and a CCD detector (D). The substrate (CS) of samples 1 (CS/R6G) and 2 (CS/PC/R6G/Au/R6G) is attached to the objective or prism via immersion oil.

Further, total internal reflection fluorescence (TIRF) measurements were performed (Fig. 1, left) where the system was built for the back focal plane (BFP) imaging. The excitation source was a 520 nm nanosecond laser beam passing through a beam splitter. A high numerical aperture objective lens (*Nikon Apo TIRF 100 \times NA 1.45*) is used to excite the sample and collect fluorescence at large angles (up to $\sim 73^\circ$). The fluorescence is collected with a forward-looking infrared (FLIR) camera (BFLY-U3-23S6M-C monochromatic), where a back focal plane image (BFP) is created after passing through two lenses. The collected light was filtered with a band-pass filter with peak transmission at 600 nm to filter out the reflected laser light and transmit the emission of a plasmonic-photonic nanostructure. In order to achieve a TIR, the incident laser beam angle must be larger than the critical angle where the incident light is coupled into an evanescent field at the cover slip (CS) and ambient interface. The TIR can be achieved by focusing the laser beam at objectives BFP, allowing the BFP imaging of fluorescence.

3. Results and discussions

In order to experimentally identify the strong coupling regime in the investigated photonic-plasmonic structures, most often the reflectance spectra of energy vs the angle of incidence are measured [29]. This allows one to transform such data to the optical dispersion $\omega(k)$. As mentioned before, the excited plasmonic resonances were sensitive to the polarization of incident light, thus, the spectroscopic ellipsometry method was used to measure the reflectance spectra of ellipsometric parameters $\Psi(\lambda)$ (polarized light ratio of amplitudes) and $\Delta(\lambda)$ (phase differences between p and s polarizations) from which the p and s polarizations were further analyzed separately. For the excitation of the SPP mode, an additional coupler is necessary, so a glass prism was used and the photonic-plasmonic structure (CS/PC/R6G/Au/R6G) was attached to the prism base. Such optical configuration in the total internal reflection is usually called total internal reflection ellipsometry (TIRE) [30, 31]. This allows one to excite a hybrid TPP-SPP mode in an ellipsometric scheme

and analyze in detail full polarization properties of such plasmon-exciton polaritonic states. The optical scheme of TIRE is presented in Fig. 1 (right). The reflection intensity of p polarization and s polarization components (taken from TIRE measurements) is shown in Fig. 2(a, b). The measured TIRE spectra (Fig. 2(a)) clearly show the splitting of TPP–SPP hybrid mode in the wavelength range where R6G dye has absorption lines (500–600 nm with a peak at 560 nm marked with a red dotted line). Meanwhile in the s-polarized reflectance spectra, only the TPP excitation coupled with R6G dye molecules (Fig. 2(b)) can be seen in the map as the SPP mode is not generated in s polarization. This indicates that for the analysis of the hybrid TPP–SPP mode coupled with R6G dye to distinguish a p-polarized reflectance component is relevant.

In order to understand the behaviour of hybrid plasmonic excitations, two plasmonic-photonic structures PC/Au and PC/PMMA/Au/PMMA were modelled with the CompleteEase software (used with a J.A. Woollam RC2 spectroscopic ellipsometer), which is based on Fresnel equations. The optical constants of the modelled layers were taken from the used software database. For the TIRE configuration, the simulated optical response of p-polarized light shows the anti-crossing of TPP and SPP resonances inside the forbidden photonic crystal band gap for both 1D PC/Au layer (Fig. 3(a)) and 1D PC/PMMA/Au/PMMA (Fig. 3(b)) modelled struc-

tures. These simulations were done in order to prove the strong coupling between the TPP and SPP plasmonic resonances and to determine the wavelength shifts in spectra due to the additional two PMMA layer. The SPP and TPP components are red shifted by 73 and 18 nm, respectively (at 47° AOI), due to the additional PMMA layers at both interfaces of the gold layer. So, any other changes in optical response were related with adding R6G dye molecules into the PMMA layer. The experimental measurements with R6G dye molecules in the PMMA matrix were conducted in the range from 40–60° AOI due to 45° of the BK7 glass prism.

As the spectroscopic ellipsometry simulations and measurements proved the presence of strong coupling as the splitting of the hybrid TPP–SPP mode dispersion curves was observed, further the same investigated samples were studied by leakage microscopy in the back focal plane optical scheme (the measurement optical scheme presented in Fig. 1, left). The optical configuration for the excitation of the samples was the same as for TIRE, the only difference was that the glass prism was replaced by an optical objective (*Nikon Apo TIRF 100×* with 1.45 NA). The emission BFP image of both the pure CS/R6G and the strongly coupled hybrid TPP–SPP mode with the R6G (CS/PC/R6G/Au/R6G) samples pumped with a 520 nm nanosecond laser can be seen in Fig. 4(a, b), respectively. Further, the cross section of the image (a red dotted

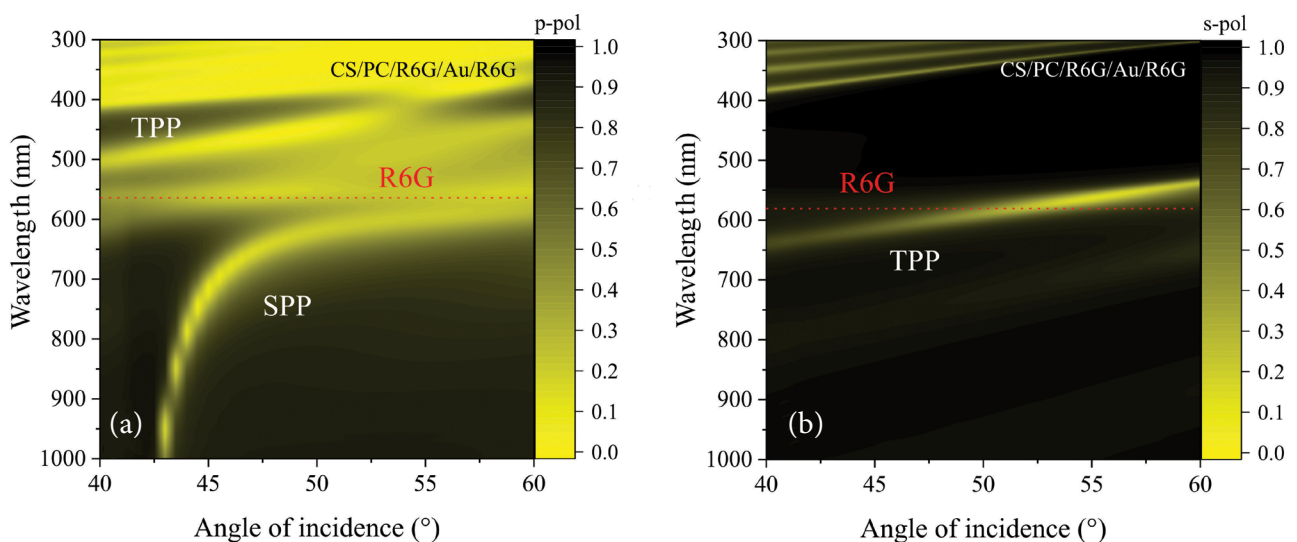


Fig. 2. Measured p polarization (a) and s polarization (b) reflection dependence on the angle of incidence in the CS/PC/R6G/Au/R6G structure supporting the hybrid TPP–SPP mode. A red dotted line marks the R6G absorption peak at 560 nm.

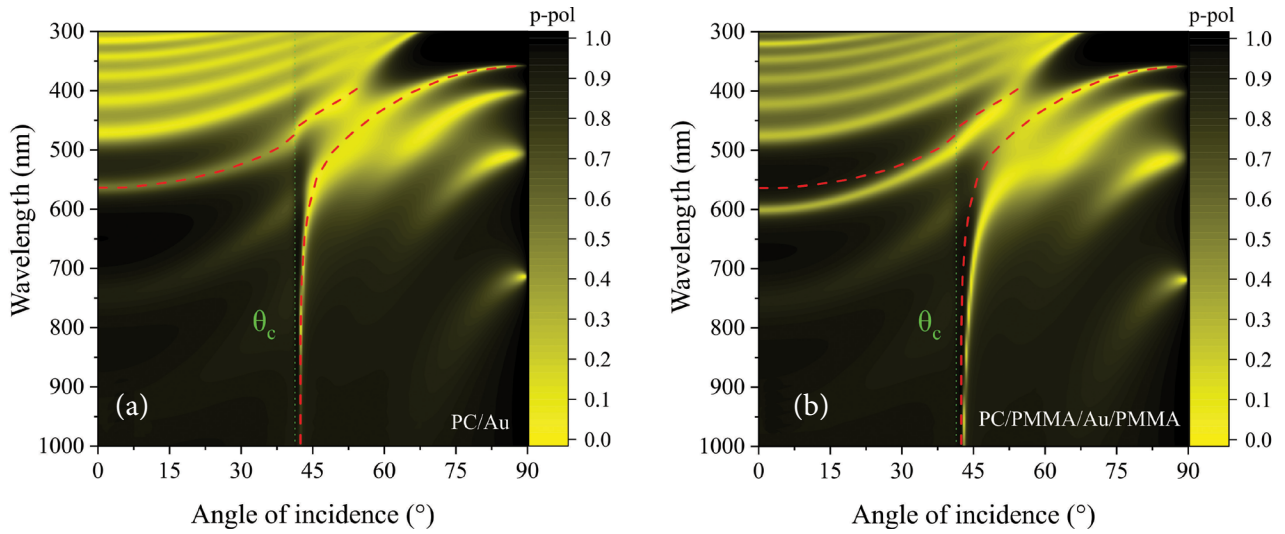


Fig. 3. Modelled p polarization reflection intensity of TPP–SPP supporting structures: (a) PC/Au and (b) PC/PMMA/Au/PMMA. Red dashed lines mark the SPP and TPP components in the PC/Au structure and a green dotted line marks the critical angle (θ_c).

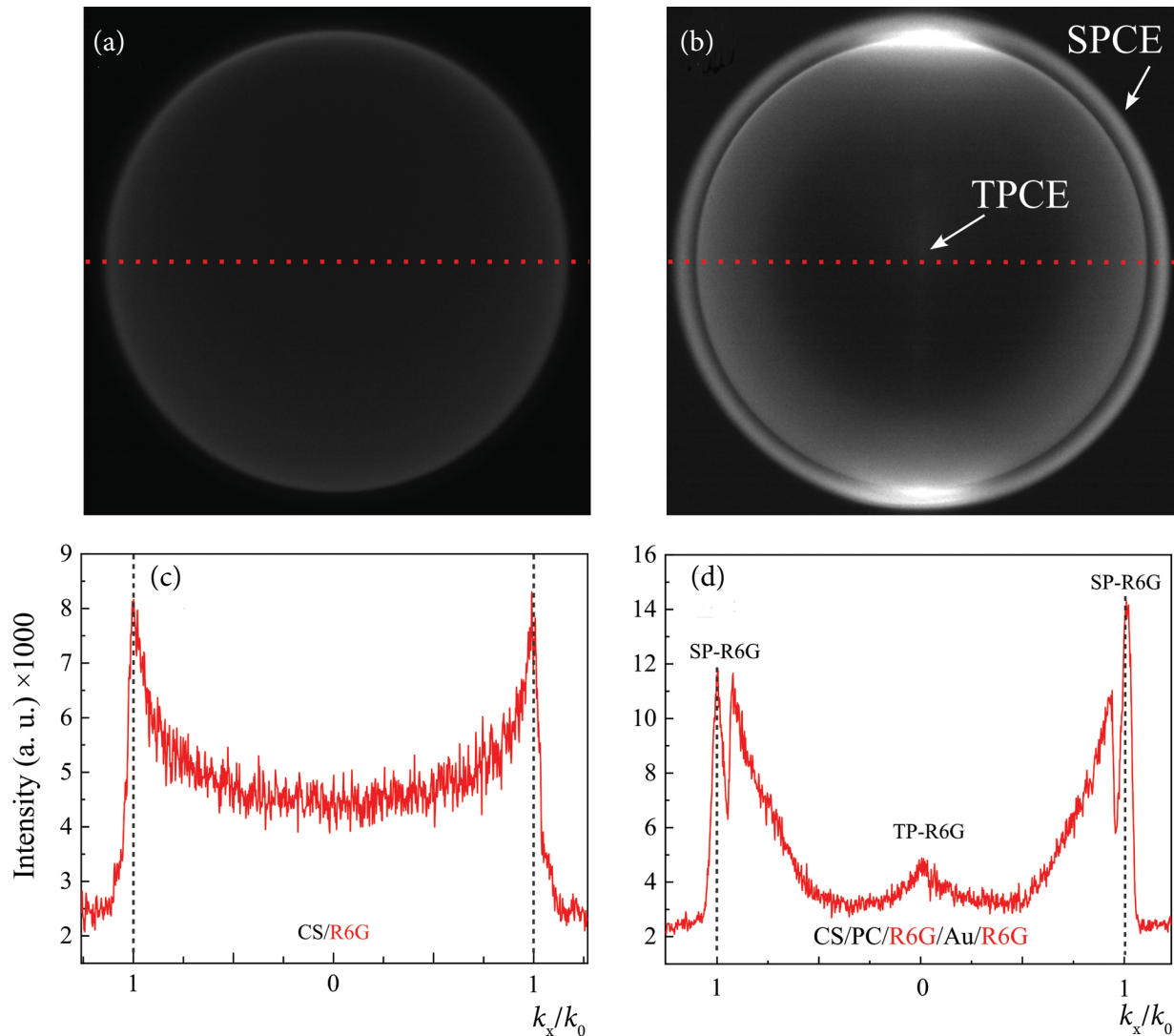


Fig. 4. Back focal plane images (a, b) of the two samples: (a) CS/R6G and (b) CS/PC/R6G/Au/R6G; the cross section of the BFP images at the red dotted line of (a) and (b), shown in (c) and (d), respectively.

line in Fig. 4(a, b)) was taken to determine the intensity distribution over the wavevector \mathbf{k} space. The cross section for CS/R6G and CS/PC/R6G/Au/R6G samples can be seen in Fig. 4(c, d), respectively. As previously, the reference sample was the pure R6G layer in the PMMA matrix deposited on the coverslip.

For the pure R6G/PMMA layer, the fluorescence emission is obtained above the critical angle when total internal reflection phenomena are achieved. From the camera view (Fig. 4(a)), a bright ring at the edge of the CS/R6G sample image can be clearly seen. This corresponds to Rhodamine 6G in the PMMA matrix emission with the highest intensity distribution at the edge of the ring (Fig. 4(c)). Meanwhile, in the strongly coupled sample (Fig. 4(b)), the outer bright ring corresponds to the SPP component in the hybrid mode and the dark ring is the critical angle for such structure. It should be noted that from the camera view the emission of TPP component is almost unnoticeable, but the cross-section of the image (Fig. 4(d)) clearly indicates weaker emission from the TPP component in the hybrid mode. The feature of R6G organic dye molecules is that their absorption and emission bands overlap due to the monomer and aggregate structure [32, 33] which depends on the concentration of dye molecules in the volume. The absorption and emission have double peaks, and such double structures can be modified and enhanced with high concentrations of molecules due to formed aggregates. Anti-crossing with peaks of both absorption lines is possible [23], indicating the formation of hybrid plasmonic modes with multiple couplings with molecule excitons. This is the case of our studies where the TPP and SPP components in the hybrid mode are strongly coupled with nearby R6G dye layers at the inner (TPP) and outer (SPP) metal/dielectric interfaces. Moreover, the tuning of emission intensities is possible by changing the metal thickness and the concentration of R6G molecules in the layer. If the metal layer thickness increases, the amount of transferred energy decreases, so in this case, we found the optimal gold layer thickness (≈ 50 nm) for such hybrid plasmonic-photonic nanostructure. Such gold layer thickness was optimal for both plasmonic resonances to efficiently excite and couple with each other,

moreover, the penetration depth at $1/e$ is about 25–30 nm for visible wavelengths. The hybrid TPP–SPP mode has an antisymmetric (TPP) and a symmetric (SPP) component. Increasing the metal layer thickness leads to weakening and broadening of the SPP, whereas the antisymmetric TPP becomes narrower. Because of that, our designed nanostructure was optimized to transfer coherent energy through the metal layer to the outer interface (SPP) and emit radiation into free space.

4. Summary

The present experimental studies have shown the strong coupling regime in the hybrid TPP–SPP mode and energy exchange between TP–R6G polariton and SP–R6G polariton components. The evidence of the energy transfer is the observation of stronger emission through the SPP component by exciting the dye molecule layer of TP–R6G from the substrate side. The main difference from the conventional spontaneous fluorescence emission of pure R6G dye is that this emission occurs due to strongly coupled extended coherent states emerging from the hybrid TPP–SPP mode and the R6G dye molecule exciton coupling. Thus, such polaritonic emission exhibits better spatial and temporal coherence properties. The hybrid plasmon-exciton polaritonic states could act as energy channels from matter-like (non-coherent) substances to light-like (coherent) modes.

The polarization-based optical methods such as spectroscopic ellipsometry are advanced optical methods with the ability to analyze in detail the strong coupling effect. The leakage microscopy method in the back focal plane is a useful tool to excite and handle plasmonic-photonic nanostructures able to radiate coherent emission from the dimensions less than the diffraction limit.

Acknowledgement

Professor Jurgis Gintautas Babonas will be dearly remembered by colleagues and his students as the first who started to use the ellipsometry method in Lithuania and laid the foundations for further development and various applications in this field.

References

- [1] P. Andrew, Energy transfer across a metal film mediated by surface plasmon polaritons, *Science* **306**(5698), 1002–1005 (2004), <https://doi.org/10.1126/science.1102992>
- [2] J. Bellessa, C. Bonnard, J.C. Plenet, and J. Mugnier, Strong coupling between surface plasmons and excitons in an organic semiconductor, *Phys. Rev. Lett.* **93**(3), 036404 (2004), <https://doi.org/10.1103/PhysRevLett.93.036404>
- [3] C. Symonds, C. Bonnard, J.C. Plenet, A. Bréhier, R. Parashkov, J.S. Lauret, E. Deleporte, and J. Bellessa, Particularities of surface plasmon–exciton strong coupling with large Rabi splitting, *New J. Phys.* **10**(6), 065017 (2008), <https://doi.org/10.1088/1367-2630/10/6/065017>
- [4] J.T. Hugall, A. Singh, and N.F. van Hulst, Plasmonic cavity coupling, *ACS Photonics* **5**(1), 43–53 (2018), <https://doi.org/10.1021/acsp Photonics.7b01139>
- [5] W.L. Barnes, Surface plasmon–polariton length scales: a route to sub-wavelength optics, *J. Opt. A* **8**(4), S87–S93 (2006), <https://doi.org/10.1088/1464-4258/8/4/S06>
- [6] T.K. Hakala, A. Moilanen, A. Väkeväinen, R. Guo, J. Martikainen, K.S. Daskalakis, H. Rekola, A. Julku, and P. Törmä, Bose–Einstein condensation in a plasmonic lattice, *Nat. Phys.* **14**(7), 739–744 (2018), <https://doi.org/10.1038/s41567-018-0109-9>
- [7] P. Berini and I. De Leon, Surface plasmon–polariton amplifiers and lasers, *Nat. Photon.* **6**(1), 16–24 (2012), <https://doi.org/10.1038/nphoton.2011.285>
- [8] A. Lishchuk, C. Vasilev, M.P. Johnson, C.N. Hunter, P. Törmä, and G.J. Leggett, Turning the challenge of quantum biology on its head: biological control of quantum optical systems, *Faraday Discuss.* **216**, 57–71 (2019), <https://doi.org/10.1039/C8FD00241J>
- [9] A. Paulauskas, S. Tumenas, A. Selskis, T. Tolenis, A. Valavicius, and Z. Balevicius, Hybrid Tamm-surface plasmon polaritons mode for detection of mercury adsorption on 1D photonic crystal/gold nanostructures by total internal reflection ellipsometry, *Opt. Express* **26**(23), 30400 (2018), <https://doi.org/10.1364/OE.26.030400>
- [10] J.A. Hutchison, T. Schwartz, C. Genet, E. Devaux, and T.W. Ebbesen, Modifying chemical landscapes by coupling to vacuum fields, *Angew. Chem. Int. Ed.* **51**(7), 1592–1596 (2012), <https://doi.org/10.1002/anie.201107033>
- [11] C.P. Dietrich, A. Steude, M. Schubert, J. Ohmer, U. Fischer, S. Höfling, and M.C. Gather, Strong coupling in fully tunable microcavities filled with biologically produced fluorescent proteins, *Adv. Opt. Mater.* **5**(1), 1600659 (2017), <https://doi.org/10.1002/adom.201600659>
- [12] J. Anulytė, V. Žičkus, E. Bužavaitė-Vertelienė, D. Faccio, and Z. Balevicius, Strongly coupled plasmon–exciton polaritons for photobleaching suppression, *Nanophotonics* **13**(22), 4091–4099 (2024), <https://doi.org/10.1515/nanoph-2024-0259>
- [13] D.G. Baranov, M. Wersäll, J. Cuadra, T.J. Antosiewicz, and T. Shegai, Novel nanostructures and materials for strong light–matter interactions, *ACS Photonics* **5**(1), 24–42 (2018), <https://doi.org/10.1021/acsp Photonics.7b00674>
- [14] Z. Jacob and V.M. Shalaev, Plasmonics goes quantum, *Science* **334**(6055), 463–464 (2011), <https://doi.org/10.1126/science.1211736>
- [15] M. Pelton, S.D. Storm, and H. Leng, Strong coupling of emitters to single plasmonic nanoparticles: exciton-induced transparency and Rabi splitting, *Nanoscale* **11**(31), 14540–14552 (2019), <https://doi.org/10.1039/C9NR05044B>
- [16] B.I. Afinogenov, V.O. Bessonov, A.A. Nikulin, and A.A. Fedyanin, Observation of hybrid state of Tamm and surface plasmon–polaritons in one-dimensional photonic crystals, *Appl. Phys. Lett.* **103**(6), 061112 (2013), <https://doi.org/10.1063/1.4817999>
- [17] M. Kaliteevski, I. Iorsh, S. Brand, R.A. Abram, J.M. Chamberlain, A.V. Kavokin, and I.A. Shelykh, Tamm plasmon–polaritons: Possible electromagnetic states at the interface of a metal and a dielectric Bragg mirror, *Phys. Rev. B* **76**(16), 165415 (2007), <https://doi.org/10.1103/PhysRevB.76.165415>

- [18] I. Tamm, Über eine mögliche Art der Elektronenbindung an Kristalloberflächen, *Z. Physik* **76**, 849–850 (1932), <https://doi.org/10.1007/BF01341581>
- [19] A. Reza, Z. Balevicius, R. Vaisnoras, G.J. Babonas, and A. Ramanavicius, Studies of optical anisotropy in opals by normal incidence ellipsometry, *Thin Solid Films* **519**(9), 2641–2644 (2011), <https://doi.org/10.1016/j.tsf.2010.12.042>
- [20] M.E. Sasin, R.P. Seisyan, M.A. Kalitchevski, S. Brand, R.A. Abram, J.M. Chamberlain, A.Yu. Egorov, A.P. Vasil'ev, V.S. Mikhlin, and A.V. Kavokin, Tamm plasmon polaritons: Slow and spatially compact light, *Appl. Phys. Lett.* **92**(25), 251112 (2008), <https://doi.org/10.1063/1.2952486>
- [21] E. Bužavaitė-Vertelienė, V. Vertelis, and Z. Balevičius, The experimental evidence of a strong coupling regime in the hybrid Tamm plasmon-surface plasmon polariton mode, *Nanophotonics* **10**(5), 1565–1571 (2021), <https://doi.org/10.1515/nanoph-2020-0660>
- [22] P. Törmä and W.L. Barnes, Strong coupling between surface plasmon polaritons and emitters: a review, *Rep. Prog. Phys.* **78**(1), 013901 (2015), <https://doi.org/10.1088/0034-4885/78/1/013901>
- [23] T.K. Hakala, J. Toppari, A. Kuzyk, M. Pettersson, H. Tikkanen, H. Kunttu, and P. Törmä, Vacuum Rabi splitting and strong-coupling dynamics for surface-plasmon polaritons and rhodamine 6G molecules, *Phys. Rev. Lett.* **103**(5), 053602 (2009), <https://doi.org/10.1103/PhysRevLett.103.053602>
- [24] P. Vasa, W. Wang, R. Pomraenke, M. Lammers, M. Maiuri, C. Manzoni, G. Cerullo, and C. Lienau, Real-time observation of ultrafast Rabi oscillations between excitons and plasmons in metal nanostructures with J-aggregates, *Nat. Photon.* **7**(2), 128–132 (2013), <https://doi.org/10.1038/nphoton.2012.340>
- [25] R. Ulbricht, E. Hendry, J. Shan, T.F. Heinz, and M. Bonn, Carrier dynamics in semiconductors studied with time-resolved terahertz spectroscopy, *Rev. Mod. Phys.* **83**(2), 543–586 (2011), <https://doi.org/10.1103/RevModPhys.83.543>
- [26] D.L. Dexter, A theory of sensitized luminescence in solids, *J. Chem. Phys.* **21**(5), 836–850 (1953), <https://doi.org/10.1063/1.1699044>
- [27] T. Förster, 10th Spiers Memorial Lecture. Transfer mechanisms of electronic excitation, *Discuss. Faraday Soc.* **27**, 7–17 (1959), <https://doi.org/10.1039/DF9592700007>
- [28] T. Förster, Zwischenmolekulare Energiewanderung und Fluoreszenz, *Ann. Phys.* **437**, 55–75 (1948), <https://doi.org/10.1002/andp.19484370105>
- [29] J. Anulytė, E. Bužavaitė-Vertelienė, V. Vertelis, E. Stankevičius, K. Vilkevičius, and Z. Balevičius, Influence of a gold nano-bumps surface lattice array on the propagation length of strongly coupled Tamm and surface plasmon polaritons, *J. Mater. Chem. C* **10**(36), 13234–13241 (2022), <https://doi.org/10.1039/D2TC02174A>
- [30] H. Arwin, M. Poksinski, and K. Johansen, Total internal reflection ellipsometry: principles and applications, *Appl. Opt.* **43**(15), 3028 (2004), <https://doi.org/10.1364/AO.43.003028>
- [31] Z. Balevicius, V. Vaicikauskas, and G.-J. Babonas, The role of surface roughness in total internal reflection ellipsometry of hybrid systems, *Appl. Surf. Sci.* **256**(3), 640–644 (2009), <https://doi.org/10.1016/j.apsusc.2009.08.033>
- [32] V.A. Kuznetsov, N.I. Kunavin, and V.N. Shamraev, Spectra and quantum yield of phosphorescence of rhodamine 6G solutions at 77°K, *J. Appl. Spectrosc.* **20**(5), 604–607 (1974), <https://doi.org/10.1007/BF00607454>
- [33] L.V. Levshin, M.G. Reva, and B.D. Ryzhikov, Structural dependence of the spectral characteristics of aggregates of complex organic molecules, *J. Appl. Spectrosc.* **34**(4), 426–431 (1981), <https://doi.org/10.1007/BF00614225>

STIPRIOSIOS SĄVEIKOS REŽIMO NULEMTA SPINDULIUOTĖ TARP HIBRIDINIŲ TAMMO-PAVIRŠINIŲ PLAZMONŲ POLIARITONŲ IR RODAMINO 6G MOLEKULIŲ EKSITONO

E. Bužavaitė-Vertelienė^{a,b}, V. Žičkus^a, J. Anulytė^a, Z. Balevičius^{a,b}

^a *Fizinių ir technologijos mokslų centro Lazerinių technologijų skyrius, Vilnius, Lietuva*

^b *Vilniaus Gedimino technikos universiteto Elektronikos fakultetas, Vilnius, Lietuva*

Santrauka

Fotoninių-plazmoninių nanostruktūrų, palaikančių hibridinius Tammo-paviršinius plazmoninius sužadimus ir jų stiprią sąveiką su rodamino 6G organinių dažų eksitonais, tyrimui taikyta visiško vidaus atspindžio elipsometrija (TIRE) ir optinė mikroskopija visiško vidaus atspindžio konfigūracijoje. Optinis TIRE atsakas parodė, kad Tammo ir paviršiaus plazmono poliaritonai stipriai sąveikauja, o hibridinis plazmoninis sužadimas lėmė rezonansų pokytį energijos spektre. Be to, tiek TPP, tiek SPP sandai hibridinėje būsenoje yra stipriosios

sąveikos režime su R6G-PMMA sluoksniais, atitinkamai esančiais 50 nm aukso sluoksnio vidinėje ir išorinėje sąsajose. Visiško vidaus atspindžio mikroskopija galinio fokuso plokštumos optinėje konfigūracijoje įrodo sužadintų emiterių energijos perdavimą per 50 nm aukso sluoksnį, kai sistema yra stipriosios sąveikos režime. Poliaritoninis spinduliavimas stipriosios sąveikos režime pasižymi geresnėmis koherentiškumo savybėmis, palyginti su įprastiniu grynu rodamino 6G organinių dažų molekulių spontaniniu fluorescencijos spinduliavimu.